Corrosion Behavior of Friction Stir Process for Al-base Nano Composite Surface Produced by Electrophoretic Deposition

The 5th International scientific Conference on Nanotechnology& Advanced Materials Their Applications (ICNAMA 2015) 3-4 Nov, 2015

Hussein A. Hussein
Production Engineering and Metallurgy Department, University of Technology /Baghdad
Email: g.hunter2008@yahoo.com

Abstract

In this study, friction stir method (FSP) was used for include walled (Al_2O_3) Nano-sized particles into the matrix of Al 5083 alloy by electrophoretic deposition (EPD). The impact of these reinforcements on microstructural modification, mechanical properties and corrosion resistance of FSP Al 5083 surface composites were studied. A rib cylindrical hardened steel tool was used with the rotation speeds of 800, 1000 and 1200 rpm and travel speeds 50 mm/min. Mechanical properties and corrosion resistance of FSP samples were evaluated and compared with the basis alloy. The corrosion behavior of the samples was investigated by potentiostatic polarization tests. Microstructural analysis accomplished by optical and SEM microscopes showed that reinforcements are well distributed within the stir zone, and grain refinement is gained. The reinforcement incremented the hardness from Hv80.083 metric weight unit for as castings to a most of Hv135.413 for friction stir. Although friction stir parameter has attenuated the corrosion current density ($7.15\mu A/cm^2$) compared to the results of the as-cast samples.

Keywords: Corrosion behavior of Friction Stir process, Microhardness, EPD.

سلوك التآكل في عملية الخلط الاحتكاكي لسبيكة الالمنيوم ذات اساس نانو التركيب المنتجه بالترسب الكهربي

الخلاصة

في هذه الدراسة، تم استخدام أسلوب الخلط الاحتكاك (FSP) للاسطح التي تشمل جسيمات من (AL_2O_3) نانوية الحجم في ارضية من سبيكة المنيوم 5083 بواسطة الترسيب الكهربي (EPD). تمت دراسة تأثير هذه التعزيزات (التقوية) على تعديل البنية المجهرية، الخواص الميكانيكية والمقاومة للتآكل للاسطح المنتجة بواسطة FSP لسبيكة 5083 المركبة السطح. تم استخدام أداة الخلط ذات شكل أسطواني من الفولاذ العدد مع سرعات دوران 800، 1000 و 1200 دورة في الدقيقة والتغذية بسرعة 50 مم / دقيقة. تم تقييم الخواص الميكانيكية والمقاومة للتآكل من عينات FSP وبالمقارنة مع سبيكة الأساس. وكان التحقيق في سلوك التآكل من العينات عن طريق اختبارات الاستقطاب potentiostatic. وأظهر تحليل البنية المجهرية بواسطة المجهرالضوئية وSEM أن تعزيزات وتوزع بشكل جيد داخل منطقة الخلط، واكتسبت صقل الحبوب.

عملية التقوية بواسطة الخلط الاحتكاكي زادت صلادة من Hv80.083 إلى أكثر من Hv135.413 مقارنة مع السبيكة الاساس. كذلك متغيرات عملية الخلط الاحتكاكي خفضت كثافة التآكل بما يقارب (μA / CM27.15) بالمقارنة مع نتائج عينات السبيكة الاساس .

INTRODUCTION

Aluminum-based metal matrix composites (MMCs) fortified with ceramic particles is attention-grabbing structural and purposeful materials. It has many advantageous properties (light weight, high stiffness, strength, superior

http://doi.org/10.30684/etj.2015.116696
2412-0758/University of Technology-Iraq, Baghdad, Iraq

wear resistance and high corrosion resistance) compared to traditional aluminum alloys and might thus be utilized in numerous industries [1,2].

However dispersion of the reinforcements during a uniform manner in metal matrix composites MMCs could be an essential and tough task. It ought to be recognized that the present process techniques for fabrication of surface composites area unit supported liquid section process at high temperatures like casting and plasma spraying [3,4]. In these cases, it's tricky to avoid the surface reaction between reinforcement and metal matrix and formation of some harmful phases. Obviously, if process of surface composite is applied at temperatures below fusion point of substrate, the issues mentioned on top of may be avoided. Recently, plentiful attention has been paid to a brand new surface modification technique named friction stir process [2,5,6].

In our recent study, a promising coating technique, (EPD) deposition could be a particulate forming process. It begins with a distributed powder material in a solvent and uses an electrical field to transference the powder particles into a desired arrangement on a conductor surface. There are four characteristics to be electrophoretic deposition process: 1. it begins with particles that are well distributed and ready to move severally in solvent suspension, 2. The particles have a surface charge attributable to electrochemical equilibrium with the solvent, 3. There is natural action motion of the particles within the bulk of the suspension, and 4. a rigid (finite shear strength) deposition of the particles is created on the deposition pole [7,8]. Frictions stir process (FSP), instituted the principle of friction stir welding, is associate rising solid state metal operating method and has tried to be a self-made technique for fabrication of hybrid Surface Metal Matrix Composites [3,4,9]. This method causes intense plastic deformation and high strain rates within the processed material leading to precise management of the microstructure through material compounding and concentration [1,10]. FSP densifies the microstructure, refines the grain size, leads to closure of porosities and provides a convenient methodology to enhance the surface properties of aluminum alloy by forming surface composites [5,10,11].

This technique has been with success used to change the microstructure of heterogeneous metallic materials, to provide surface composites, and to synthesize composites and intermetallic compounds [12, 10]. The 5083Al alloy is often utilized in construction, rail cars, vehicle bodies, mine skips and cages, pressure vessels, TV towers and drilling rigs [13]. Previous study investigates the result of doping the surface of 5083 Al with Nano-sized assail particles through friction stir process on its mechanical behavior viz. microhardness and wear resistance [14].

Byung-Wook AHN et al (2012) pointed out that the influence of the number of FSW passes on the distribution of SiC particles and mechanical properties in the joint. After one pass, the SiC particles were entangled in the upper side of the stir zone (SZ), Dharmpal Deepak et al (2013) focused on fabrication of surface composite based on 5083Al matrix reinforced with nano-sized silicon carbide particles by Friction stir processing (FSP), S.A. Hosseini et al (2015) investigated of friction stir processing (FSP) was utilized to incorporate Multi Walled Carbon Nano Tubes (MWCNT) and nanosized cerium oxide particles into the matrix of Al5083 alloy to form surface reinforced composites and W.Y. Li et al (2015) studied aluminum coating was deposited on the surface of a friction stir welded 2024-T351 aluminum alloy joint via cold spraying for corrosion protection.

In this work, (Al_2O_3) particles were deposited on 5083 via FSP for the aim of up the mechanical properties and corrosion behavior of the joint. The 5xxx series alloys are at most work hardenable alloys and their microstructure, typical of rolling/work hardening that's the most contributor to the high hardness of the basis metal (BM) compared to base alloy.

Experimental Procedure

Material

The staple utilized in this study was 5083-Al alloy in dimensions (Length:140mm, Width:15mm, Thickness:7mm) has been elected for the aim of concluding FSP. And its chemical composition is shown in Table, as calculable through qualitative analysis technique.

Table (1) Chemical composition (wt. %) of alloy used in this study

Element	Si	Fe	Cu	Mg	Zn	Mn	Al
Content (wt.%)	0.04	0.17	0.03	2.78	0.063	0.97	Rest.

Material deposition: the fabric employed in the deposition method (Al_2O_3) nano particle size ≈ 50 nm type MKN- A040 USA.

Preparation of (Al_2O_3) layer:

The surface of 5083 Al plate is doped through FSP with nano-sized (Al_2O_3) powder by electrophoreses deposition (EPD) was carried with electric field applied between associate metal counter conductor (anode) and metal alloy (cathode). EPD was performed at the lab temperature applied voltages 50V and deposition times of 6 minutes. The cell consisted of 5g/L aluminum oxide (Al_2O_3) aquatic dispersion of nanosized particles, suspended in Ethanol with distilled water. Powder suspension was ready by magnetic stirring of the mixture of ceramic powders in alcohol for thirty min. it was followed by a high-energy sonication before deposition; the coatings were dried at 50C˚. Fig. (1) shows the surface of 5083Al plate after (Al_2O_3) deposition.

Figure (1) the surface of 5083 Al plate after alumina (Al_2O_3) deposition.

Friction stir process

The construct used for implementing friction stir process consists of a standard vertical milling machine and a specially designed rotating FSP tool as shown in Fig. (2a). The specimens were mounted with rigid clamping device to obstruct from moving out of position. The process tool was made from high steel (type H13) with

cylindrical-shouldered and rib pin. The diameter of the shoulder was 16mm; and therefore the diameter of the pin was 4 mm and 4 mm height as shown in Fig (2b).

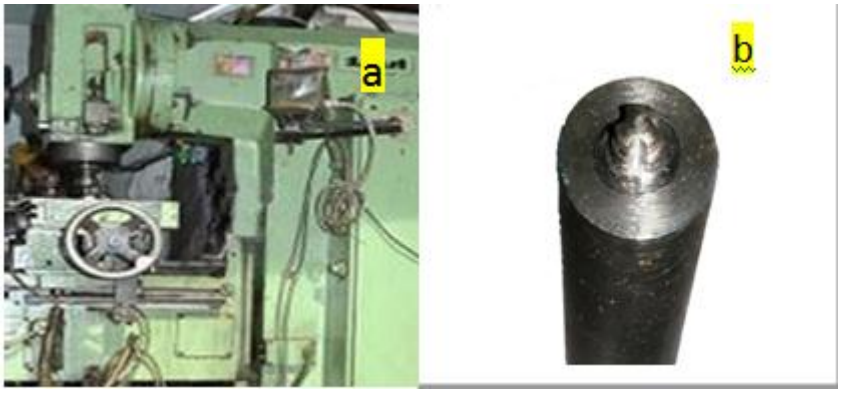

Figure (2) Equipment for friction stir processing: (a) milling machine of friction stir processing. (b) The FSP tool.

After the plates are fixed properly, it began the process by rotating the tool (cylindrical-shouldered and rib pin), and plunging the pin into the work piece till the shoulder created full contact with work piece surface at a degree on the process line. Friction stir processing has been performed by using different tool rotation speeds of (800, 1000, and 1200) rpm and travel speeds 50mm/min. Figure (3 a,b) shows some process specimens.

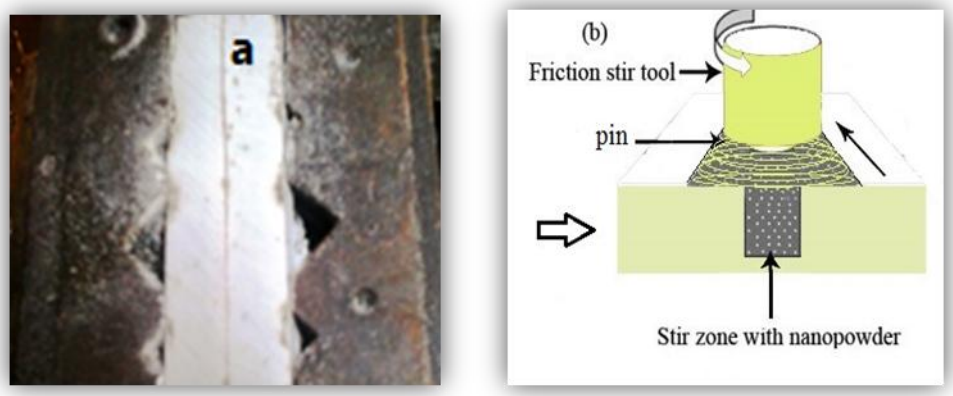

Figure (3) Fixture specimen

As the tool progressed on the middle line of the trained holes, a layer of 5083Al-(Al_2O_3) nano-composites was stired on the surface of base plate (Fig. 4).

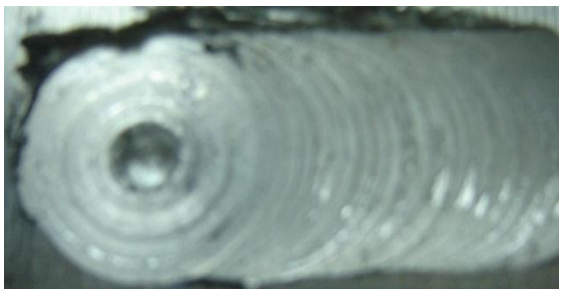

Figure (4)The processed specimens.

Testing investigation.

Microstructural Examination:

Optical microscopy and SEM were utilized to test the morphology and different probable localized attacks in numerous regions of FSP samples. The transversal cross section of joint was neatly applying customary metallographic techniques consisting of grinding with burnish 320, 500,600, 800, 1000, 1200 and 3000 abrasive paper, followed by scrubbing and etching in a proper etchant solution composed of hydrofluoric (40 vol.%), hydrochloric (37 vol.%), nitric (65 vol.%) acids in distilled water till the various regions of the welded samples were roughly observable during optical microscopy observations.

Microhardness Measurement

Microhardness of the friction stir processed samples was measured at numerous locations, starting from the processed zone to base metal, with the assistance of Vicker's microhardness tester. The hardness measurements were taken on the surface of samples at associate interval of 2mm, on each side of center line of FSP zone. The microhardness of the basis alloy was measured in a very similar fashion. The dimensions of indentation was measured with the assistance of a micrometer associated a lens having magnification of the order 10X, fitted on the hardness tester. The indentation marks were created with the assistance of a pyramid form diamond indenter at a load of 20 gram and dwell time of around 10 sec.

Wear Rate Measurement

Pin-On-Disc wear equipment was used, that was designed consistent with ASTM specification F732-82[13]. The wear equipment consists of motor with constant revolution speed (510 rpm). Weight technique was wont to verify the wear rate of specimens. The specimens were weighted before and after the wear test by sensitive balance sort (DENVER instrument) (Max-210gm) with accuracy 0.0001 gm. The weight loss (ΔW) was divided by the skid distance and therefore the wear rate was obtained by Utilization equation as follows:-

$$\text{Wear rate} = \frac{\Delta w}{SD} \quad \dots (1)$$

$$\Delta w = w_2 - w_1 \quad \dots (2)$$

$$SD = SS * t \quad \dots (3)$$

$$\text{Wear rate (W.R)} = \frac{\Delta W}{\pi D.N.t} \quad \dots . (4)$$

Where:
SD = linear skid speed (m/sec.)
D = skid circle diameter (cm)
t = skid time (min)
N = steel disc speed (rpm)
Hardness of steel disc =50 HRc
Diameter of specimen =10mm
Length of specimen = 15mm

Corrosion Test

Electrochemical investigation of the 5083Al was performed with potentiostatic polarization. All experiments were accomplished with a computer-controlled potentiostatic (PCI4/750, GAMRY Instruments, Inc., Warminster, PA) in 3.5% NaCl solution at room temperature. Ag/AgCl and (Pt) electrodes were used as a reference and auxiliary electrode, respectively as shown in Fig.(5). Specimens were immersed into the solution till getting a steady open circuit potential (OCP). The exposed area of the test specimens was about 10 mm^2. Impedance parameters were calculated by fitting the experimental results to an equivalent circuit model by using the Echem Analyst software.

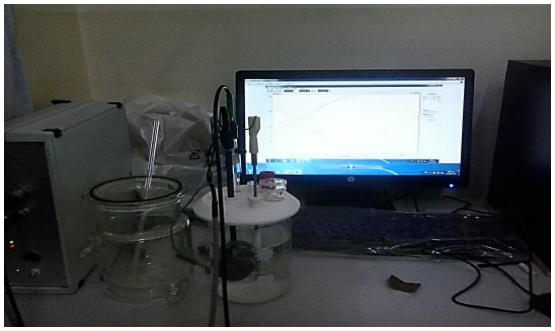

Figure (5).The electrochemical corrosion unit.

Results and Discussion

Microstructural observations

The macrostructures of the (Al_2O_3)/ 5083 alloy composites made by FSP ar shown in Fig. 6 consistent with the FSP conditions. Dispersion of the (Al_2O_3) particles within the Al-alloy matrix was associated at the rotation speeds of FSP processes [15]. During this case one pass of FSP method, criss-cross Al_2O_3 particles may well be seen within the center of the joint, the Al_2O_3 particles were spread a lot of homogeneously connected with the rise rotation speeds of the stir method. Fig. (6) shows the microstructure of the stir zone made below the various FSP rotation speeds the microstructure of the stir zone fashioned below the various FSP conditions[14,15].

As metals containing particles underwent hot deformation, the particles usually play a very important role within the dynamic recrystallization of the matrix materials [16]. The promise impact is wherever the particles pin the movement of the grain boundary and retard the grain growth once dynamic recrystallization [13]. The FSP with the Al_2O_3 particles is taken into account to create fine grains a lot of impact attributable to the promise effect of the Al_2O_3 particles.

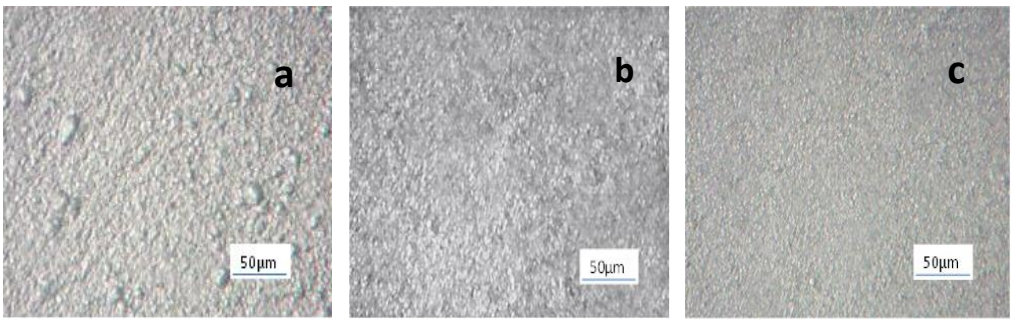

Figure (6) Optical micrographs of joint in several rotation speeds: (a) at 800 rpm; (b) at 1000 rpm and (c) at 1200 rpm.

Fig. (6) shows the rate nanoparticle agglomeration sizes within the sample obtained from the stir zone of specimens. As shown within the figure, with increase of spinning speed, the common grain size of the composite will increase attributable to higher heat generation. Fig. (7) shows the SEM pictures of the samples, wherever particle distributions are visible. Then, the tool passes, the nanoparticle agglomeration size reduced and therefore the reinforcement distribution is improved [14,16]. Breaking the onion ring formed agglomeration fashioned at the previous FSP pass and additional separation of the nanoparticle agglomeration resulted in improved nanoparticle distributions. As spinning speed accretion, the nanoparticle agglomeration size of alumina nanoparticles ablated attributable to increase in material flow within the stir zone [2,5,9,17].

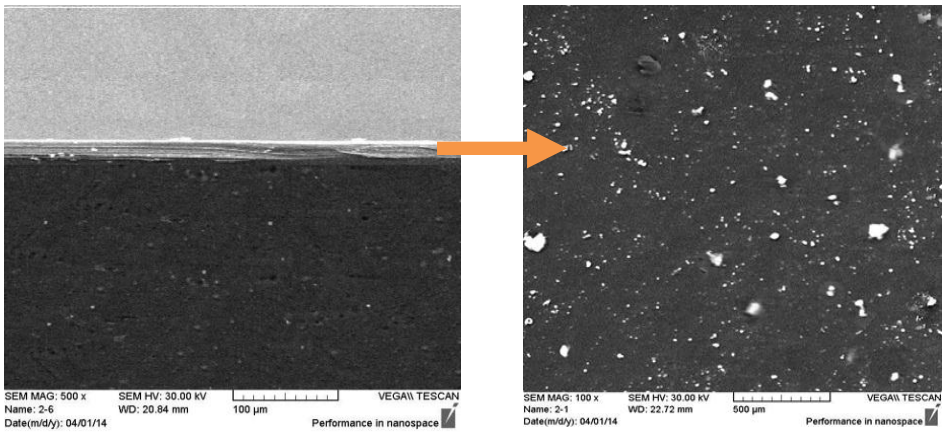

(a) at 800 rpm

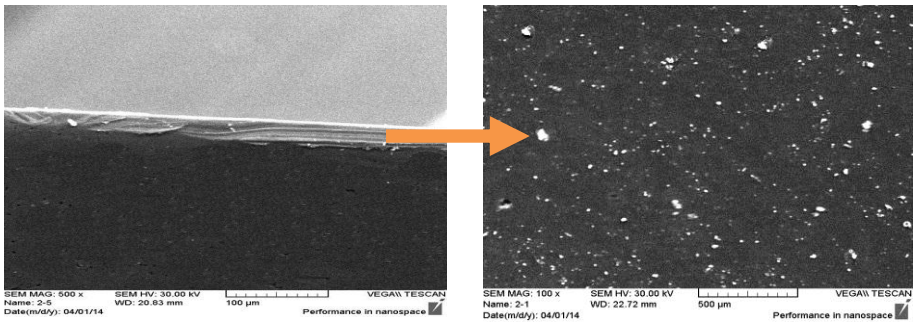

(b) at 1000 rpm

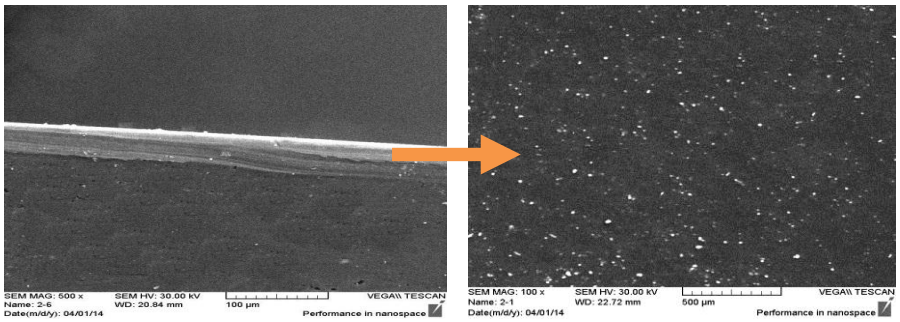

(c) at 1200 rpm.

Figure (7) SEM images of cross section of FSP samples (a) at 800 rpm; (b) at 1000 rpm and (c) at 1200 rpm.

Microhardness Profile

The Vicker's microhardness distributions in specimens on each side of the weld interface are shown in Fig (8). The measurements were implementing each within the central axis and along the line located 2.5 mm from the surface. It clearly shows that microhardness amount of the FSP base alloy without reinforcement was increased in gas compared with the as-received alloy, expected to be due to grain refinement and also due to fragmentation and distribution of second phase intermetallic particles [9,11]. The rise in hardness values was obviously higher in composites strengthened with Al_2O_3 particles. Here, the impact are going to be a lot of pronounced since reinforcements are in Nano scale and well distributed by FSP. Secondly, it's attributable to the impact of microstructural modification in nugget zone NZ. It's acknowledged that grain size refinement will enhance the hardness. It's additionally believed that homogenized distribution of Nano sized reinforcement, results in pinning of dislocations and retarding grain growth [11,13,15]. hardness is 106 HV which means it's quite double more durable than the basis alloy that possesses a hardness of less 80 HV. Indeed, for the FSP composites with higher weight ratios of reinforcements, agglomeration will occur that disturbs the uniform distribution of particles and makes the variation in hardness profile. In these cases, the role of reinforcement and their distribution have also to be taken under consideration [18].

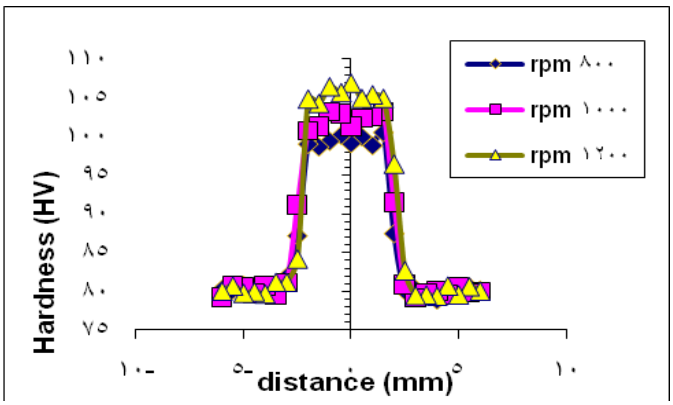

Figure (8): Hardness profile along centerline of cross-section of FSP processed.

Corrosion behavior of FSP

The corrosion rates were calculated and also the results are conferred in Fig. (9). It had been ascertained that because the spinning speed increased, the corrosion rate decrease [4,12,19]. Thus, the spinning speeds have a direct relationship with the corrosion rate. When the spinning speeds were increased from 800 rpm to 1200 rpm, the corrosion current density (corrosion rate) was decreased compared with corrosion current density for as-received sample. It's attention-grabbing to notice that for a particular spinning speed, all-time low corrosion resistance was ascertained at the most spinning speed for the sample [3,20].

Increasing spinning speed at 800 and 1000 rpm led to shift corrosion potential to more noble direction, while the spinning speed of 1200 rpm shifted the E_{corr} toward noble direction compared with as-received sample as shown in Table (2).

Some phenomena decelerating the passivity and heartening the localized corrosion. (e.g., intermetallic phases like Al_3Mg_2 have less noble dissolution potential relative to Al matrix and act as anodal spots [20,21]. Obviously, the pitting corrosion resistant on grain boundaries will be seen within the metallographic examination in Fig. 10. It a lower pitting corrosion with increase speeds (as shown in Fig. 10c); but, higher pitting attack within the stir zone will clearly be seen at 800 and 1000 rpm (Fig. 10a and b). The most corrosion attack is appeared as pitting corrosion within the stir zone SZ as results of the dominant dissolution of Al-Mg intermetallic networks around grains [9].

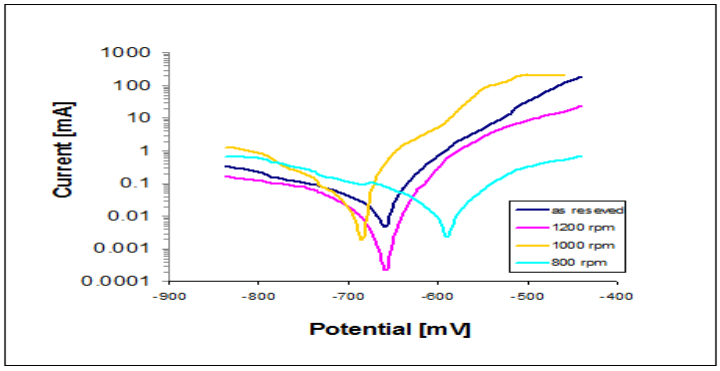

Figure (9): Potentiostatic polarization curves of the as-received and FSP samples with different rotation speeds in 3.5% NaCl solution.

Table (2) Polarization diagram parameters in 3.5g/L NaCl for stir zones of FSP 5038.

Samples	E_{corr} (mV)	i_{corr} (mA/cm^2)
As received	676.1-	16.18
FSP sample at 800 rpm	-602.5	14.51
FSP sample at 1000 rpm	-672.2	12.21
FSP sample at 1200 rpm	-685.9	9.03

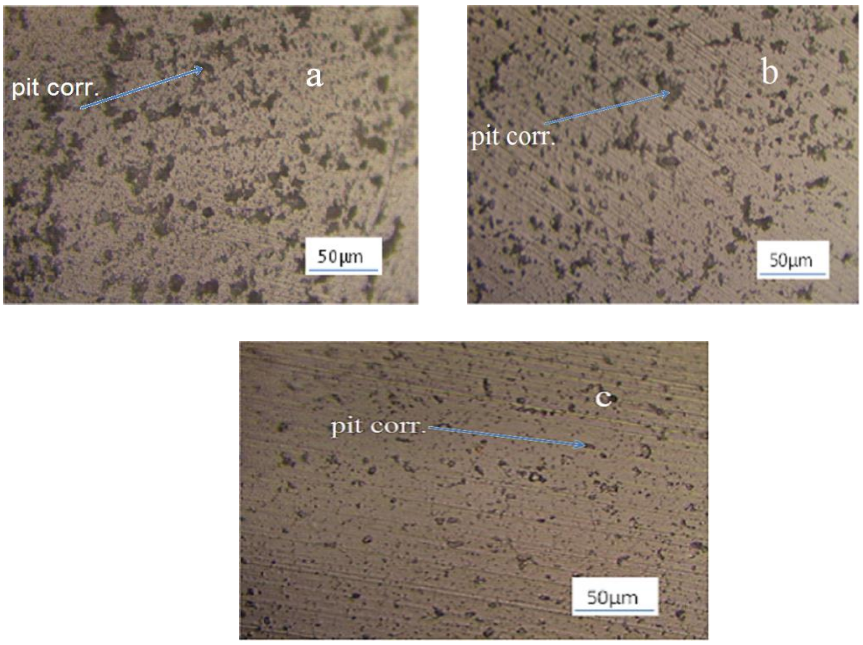

Figure (10) images of surface of FSP samples after corrosion in 3.5% NaCl solution: (a) at 800 rpm; (b) at 1000 rpm and (c) at 1200 rpm.

Wear behavior of FSP

Figure (11) shows the variation of wear rate as a perform of slip distance for friction stir processed Al/Al_2O_3 composites. It is seen that because the slippy distance will increase, the wear and tear rate decreases for all applied traditional masses. The wear and tear rate of friction stir processed composites is considerably lower as compared to spinning speed for applied traditional masses. Also, the wear and tear rate of processed composites decreases with increasing tool rotation speed of constant traditional load and slippy distance. The improved wear resistance thanks to fiction stir process is attributed to the distribution of reinforcing Al_2O_3 particles within the matrix and refinement of Al-grain.

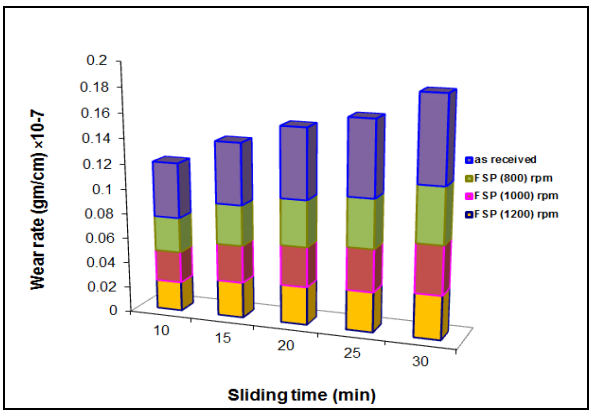

Figure (11): The variation of wear rate with sliding time at different rotation speeds.

Fig.(12) shows SEM micrograph of worn surface of stir processed composites. The micrograph reveals that the worn track breadth decreases in friction stir space compared to unprocessed space. it's proof that the extent of wear and tear in FSP composite is below that of unprocessed stir. The depth and breadth of the grooves generally imply that Associate in foster quantity of fabric off from the specimen surface [16]. it is expected that uniform distribution of Al_2O_3 particles and modification of Al-grains can cause a high wear resistance.

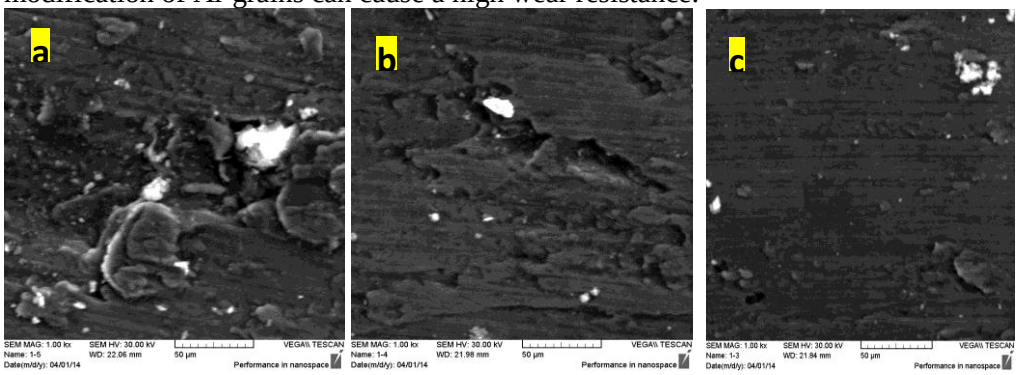

Figure (12) Scanning electron micrographs of worn track: (a) at 800 rpm; (b) at 1000 rpm and (c) at 1200 rpm.

Conclusions

1) The distribution of Al_2O_3 particles in the SZ after processing was more homogenous with increase spinning speed.

2) The grain size of the SZ with Al_2O_3 particles was smaller than that of the SZ without Al_2O_3 particles due to the pinning affected by the Al_2O_3 particles.

3) The microhardness and wear resistance of the SZ with Al_2O_3 particles was higher than that of the SZ without Al_2O_3particles due to the reduction in the grain size and the presence of the reinforcingAl_2O_3 particles in the aluminum matrix.

4) The corrosion parameters of FSP were influenced by stir processing parameters. The corrosion resistance increased with increasing spin speed.

References

[1] B.Wook, D. Choi, Y.Hwan Kim, S.Jung "Fabrication of SiCp/AA5083 composite via friction stir welding" School of Advanced Materials Science and Engineering, Sungkyunkwan University, Trans. Nonferrous Met. Soc. China 22(2012) s634−s638.

[2] M. Sharifitabar , A. Sarani, S. Khorshahian, M. ShafieeAfarani "Fabrication of 5052Al/Al_2O_3nanoceramic particle reinforced composite via friction stir processing route" Materials Science and Engineering Division, Zahedan, Iran, Materials and Design 32 (2011) 4164–4172.

[3] E. T. Akinlabi, A. ANDREWS, S. A. Akinlabi "Effects of processing parameters on corrosion properties of dissimilar friction stir welds of aluminum and copper" Trans. Nonferrous Met. Soc. China 24(2014) 1323−1330.

[4] M. Bagheri Hariri, S. Gholami Shiri, Y. Yaghoubinezhad , M. MohammadiRahvard "The optimum combination of tool rotation rate and traveling speed for obtaining the preferable corrosion behavior and mechanical properties of friction stir welded AA5052 aluminum alloy" Materials and Design 50 (2013) 620–634.

[5] M. Salehi, M. Saadatmand, J. aghazadeh "Optimization of process parameters for producing AA6061/SiC nanocomposites by friction stir processing" Trans. Nonferrous Met. Soc. China 22(2012) 1055−1063.

[6] M. Assidi, L.Fourment, S.Guerdoux, T.Nelson "Friction model for friction stir welding process simulation: Calibrations from welding experiments" International Journal of Machine Tools & Manufacture 50 (2010) 143–155.

[7] A. R. Boccaccini, S. Keim, R. Ma, Y. Li and I. Zhitomirsky, J. R. Soc. "Electrophoretic deposition of biomaterials"Interface 2010 7, S581-S613 first published online 26 May 2010.

[8] J. J. Van Tassel "Electrophoresis Deposition Fundamentals, Mechanisms and Examples With An In Depth Examination Of The Ion Depletion Effect" Materials Science and Engineering ,The Pennsylvania State University, The Graduate School, College of Earth and Mineral Sciences, 2009 Ph.D. Thesis.

[9] P. Dong, D. Sun, B. Wang, Y. Zhang, H.i Li "Microstructure, microhardness and corrosion susceptibility of friction stir welded AlMgSiCu alloy" Materials and Design 54 (2014) 760–765.

[10] P. Prakash, S. Kumar Jha, S. Prakash "A Study Of Process Parameters Of Friction Stir Welded AA 6061 Aluminum Alloy" International Journal of Innovative Research in Science, Engineering and Technology Vol. 2, Issue 6, June 2013.

[11] D. Deepak, R. Singh Sidhu, V.K Gupta "Preparation OF 5083 Al-SiC Surface Composite By Friction Stir Processing And Its Mechanical Characterization" International Journal of Mechanical Engineering, Volume 3 Issue 1, January 2013.

[12] W.Y. Li, R.R. Jiang, C.J. Huang, Z.H. Zhang, Y. Feng "Effect of cold sprayed Al coating on mechanical property and corrosion behavior of friction stir welded AA2024-T351 joint" Materials and Design 65 (2015) 757–761.

[13] S.A. Hosseini, K. Ranjbar, R. Dehmolaei , A.R. Amirani "Fabrication of Al5083 surface composites reinforced by CNTs and cerium oxide nano particles via friction stir processing" Journal of Alloys and Compounds 622 (2015) 725–733.

[14] I. Boromei, L. Ceschini, A. Morri, L. Garagnani "Friction Stir Welding Of Aluminum Based Composites Reinforced With Al_2O_3 Particles: Effects On Microstructure And Charpy Impact Energy" Metallurgical Science and Technology,

[15] Y. X. Gan, D. Solomon and M. Reinbolt "Friction Stir Processing of Particle Reinforced Composite Materials" Materials 2010, 3, 329-350.

[16] M. Antony, B. T. Pavithran, I. Thamban "Friction Stir Processing of AA6061 –A Study" College of Engineering, Kothamangalam, International Journal of Emerging Technology and Advanced Engineering, Volume 3, Issue 1, January 2013) 589.
[17] B.T. Gibson, D.H. Lammlein, T.J. Prater, W.R. Longhurst, C.D. Cox, M.C. Ballun, K.J. Dharmaraj, G.E. Cook, A.M. Strauss "Friction stir welding: Process, automation, and control" Journal of Manufacturing Processes 16 (2014) 56–73.
[18] A. Baradeswaran, A. ElayaPerumal "Study on mechanical and wear properties of Al 7075/Al_2O_3/graphite hybrid composites" Composites: Part B 56 (2014) 464–471.
[19] H. S. Patil, S. N. Soman "Corrosion Behaviour of Friction Stir Welded Aluminium Alloys AA6082-T6" American Journal of Materials Engineering and Technology, 2014, Vol. 2, No. 3, 29-33.
[20] M. Abdulstaar, M. Mhaede, L. Wagner, M. Wollmann "Corrosion behaviour of Al 1050 severely deformed by rotary swaging" Materials and Design 57 (2014) 325–329.
[21] D.Raguraman, and L.K.Kumaraswamy Dhas "Corrosion Study in Friction Stir Welded Plates of AA6061 and AA7075" International Journal of ChemTech Research CODEN (USA): IJCRGG ISSN : 0974-4290 Vol.6, No.4, pp 2577-2582, July-Aug 2014.